Vol. 543: 89–106, 2016
doi: 10.3354/meps11562

MARINE ECOLOGY PROGRESS SERIES
Mar Ecol Prog Ser

Published February 3

Cell viability, pigments and photosynthetic performance of Arctic phytoplankton in contrasting ice-covered and open-water conditions during the spring–summer transition

Eva Alou-Font[1,3,*], Suzanne Roy[1], Susana Agustí[2], Michel Gosselin[1]

[1]Institut des sciences de la mer (ISMER), Université du Québec à Rimouski, 310 Allée des Ursulines, Rimouski, Québec G5L 3A1, Canada

[2]Red Sea Research Center, King Abdullah University of Science and Technology, KAUST, Thuwal, 23955-6900, Kingdom of Saudi Arabia

[3]*Present address:* Balearic Islands Coastal Observing and Forecasting System, SOCIB, ParcBit, 07121, Mallorca, Spain

ABSTRACT: We examined phytoplankton biomass and community composition (mostly based on pigments) as well as cell viability with the cell digestion assay in surface waters of the Canadian Beaufort Sea during the spring–summer transition. Our aim was to understand phytoplankton responses to the large environmental changes (irradiance, temperature and nutrients) occurring during this period. Two categories of stations were visited in May and June 2008: ice-covered (IC), exposed to low irradiances, and open-water (OW), exposed to higher irradiances. We observed a large variation in the percentage of living cells (%LC) relative to the total community. No relationship was found between %LC and nitrate concentration (the nutrient potentially limiting in this environment). The *in situ* irradiance influenced the status of the cells at OW stations. Mean surface mixed layer irradiances >600 µmol photons m^{-2} s^{-1} were associated with low cell viability and a decline in photosynthetic performance (F_v/F_m). For IC stations, %LC declined at temperatures above 0°C, whereas for OW stations, it increased, suggesting that ice melting resulted in the release into surface waters of unhealthy cells from the bottom ice in one case, and that seasonal warming favored the communities present in open waters. A chlorophyll degradation pigment tentatively identified as pyropheophorbide *a*-'like' showed a significant negative relationship between its concentration (relative to chlorophyll *a*) and the %LC and F_v/F_m. Our results suggest that the melting conditions influence the distribution of this pigment and that it may be useful as a marker for low cell viability of ice algae being released into surface waters.

KEY WORDS: Arctic · Cell viability · Photosynthetic performance · Pigments · Sea-ice melt

INTRODUCTION

Seasonal variations in solar radiation and sea-ice cover have a large influence on primary production in the Arctic (Gosselin et al. 1990, Rysgaard et al. 1999, Mundy et al. 2011). Pelagic production is maximal in the summer months between sea-ice melt in spring and freeze-up in fall (Horner & Schrader 1982, Wang et al. 2005, Tremblay et al. 2012). With the current global change in climate, some researchers predict that the annual phytoplankton production in the Arctic Ocean will be enhanced due to the decrease of the minimum summer ice extent that could result in a longer phytoplankton growing season (Arrigo et al. 2008, Zhang et al. 2010). However, during the summer, the freshwater inputs from rivers and ice melt-

*Corresponding author: ealou@socib.es

ing (Macdonald et al. 2004, Peterson et al. 2006) can lead to strong stratification of the water column, especially if this is enhanced by the increase of river inflows (Peterson et al. 2002), which could lead to a depletion of nutrients in the surface layer (Tremblay & Gagnon 2009) and to the exposure of phytoplankton to higher irradiances. The accelerated changes in the Arctic caused by sea-ice cover decline (Stroeve et al. 2007, Comiso et al. 2008, Overland & Wang 2013) and the rapidity of the melting will influence the new conditions to which cells are exposed.

Recent studies have focused on the responses of the algal community to some of these modifications (Li et al. 2009, Tremblay et al. 2012), including the effects of changes in light (La Rocca et al. 2015), temperature (Coello-Camba et al. 2014), salinity (Hernando et al. 2015) and nutrients (van de Poll et al. 2005) and their coupled effects (Petrou & Ralph 2011, Rajanahally et al. 2014) on the physiology and viability of polar species. However, there is still much uncertainty about how the algal community will adjust to ongoing changes in environmental conditions (e.g. sea-ice coverage, light and nutrient availability, and water temperature). Knowledge about cell viability under these changing conditions could help us understand their influence on the physiology of phytoplankton cells and the dynamics of phytoplankton populations, but this is rarely studied in field programs and few data are available from the Arctic (Llabrés & Agustí 2008, Lasternas & Agustí 2010, Echeveste et al. 2011). Field studies in regions other than polar environments have highlighted a high proportion of dead cells, especially in surface waters (van Boekel et al. 1992, Hayakawa et al. 2008) and in oligotrophic environments (Agustí 2004, Alonso-Laita et al. 2005, Alonso-Laita & Agustí 2006). Some studies looked for marker compounds that could provide information on cell viability, such as chlorophyll *a* (chl *a*) degradation products that are produced during the processes of senescence and death of the cells (Spooner et al. 1994, Szymczak-Żyła et al. 2008). These degradation pigments could be useful as markers for the loss of cell viability (Franklin et al. 2012).

The overall objective of this study was to investigate phytoplankton cell viability and other cell health indicators in the Canadian Beaufort Sea during the spring–summer transition. The specific objectives were to (1) examine the variability in phytoplankton cell viability, specifically over the ice-melt period in spring, (2) identify factors contributing to the loss of viability, if any, such as high irradiance or nutrient depletion, and (3) examine signs of a decline in physiological condition of the algae, such as low photosystem II (PSII) efficiency or an increase in degradation pigments.

MATERIALS AND METHODS

Study site and sampling

This study was conducted in the Canadian Beaufort Sea (Fig. 1), as part of the International Polar Year–Circumpolar Flaw Lead system study (IPY–CFL; Barber et al. 2010), onboard the Canadian Coast Guard Ship (CCGS) 'Amundsen.' Water samples (n = 66) were collected from 29 April to 13 July 2008. Stations visited included ice-covered (IC) and open-water (OW) sites (Fig. 1). First-year drifting sea-ice stations were located in the Amundsen Gulf, whereas first-year landfast ice stations were situated in Franklin and Darnley Bays and at the entrance to M'Clure Strait (northwestern Banks Island; Fig. 1). After 24 June, Franklin Bay stations were free of ice.

At each station, vertical profiles of water temperature, salinity, photosynthetically active radiation (PAR, 400 to 700 nm) and *in vivo* fluorescence were measured using an SBE-911*plus* CTD probe (Sea-Bird Electronics) equipped with a QCP-2300 PAR sensor (Biospherical Instruments) and an *in situ* fluorometer (Seapoint Sensor). The probe and sensors were mounted on a rosette equipped with twenty-four 12 l Niskin-type bottles (Ocean Test Equipment). A vertical PAR profile was also created with a PNF-300 radiometer (Biospherical Instruments) at OW stations. The vertical profiles of irradiance from the irradiance sensor on the rosette and from the PNF-300 radiometer were used to estimate the diffuse attenuation coefficient of downwelling PAR (K_d, m^{-1}) at IC and OW stations, respectively. *In situ* PAR at the sampled depth (E_z) was calculated using Beer's law as:

$$E_z = E_0 e^{-K_d Z} \quad (1)$$

where E_0 is the PAR value at the ice–water interface for IC stations and at the sea surface for OW stations (µmol photons m^{-2} s^{-1}) and Z is the sampled depth (m).

Downwelling incident PAR irradiance was measured at 1 min intervals with a PARLite™ quantum sensor (Kipp & Zonen) installed on a tower at the bow of the ship. These data were used to calculate daily incident PAR.

The surface mixed-layer depth (Z_m) was determined as the depth for the shallowest extreme curvature of density (sigma-t, σ_t) and temperature profiles (de Boyer Montégut et al. 2004; Table 1). An index of

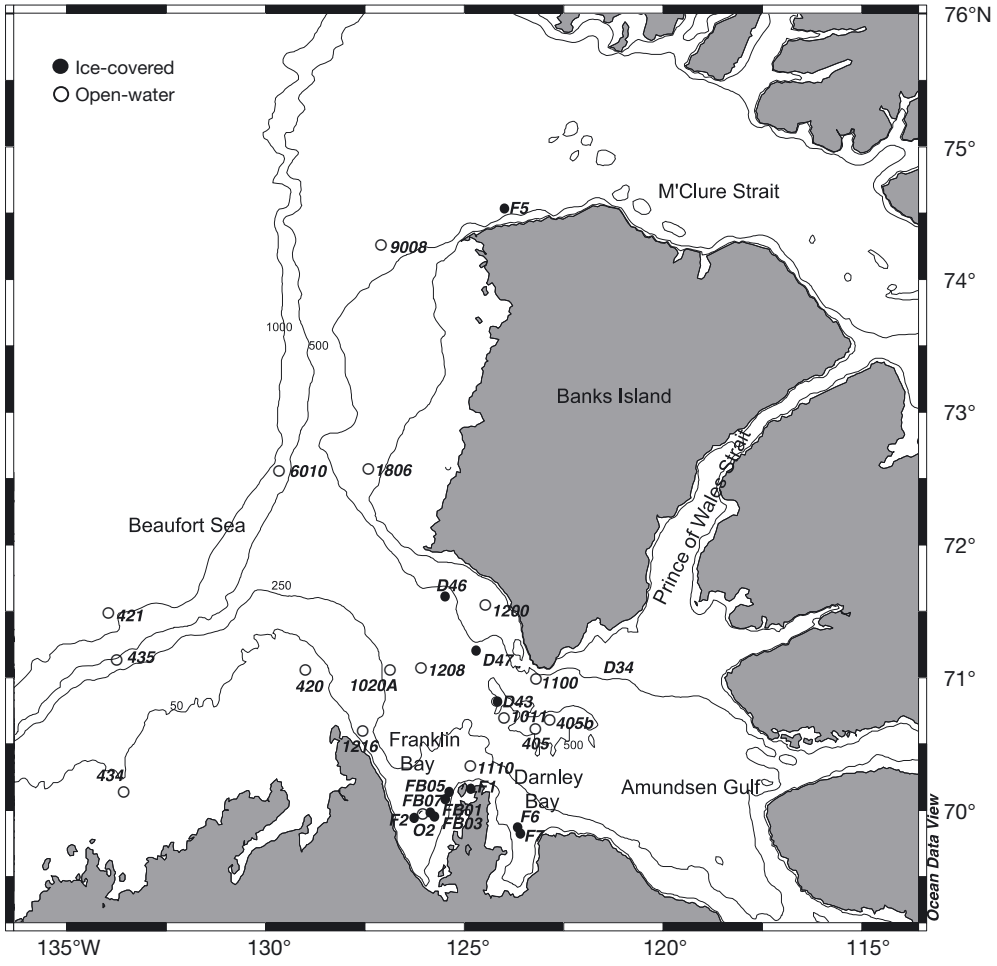

Fig. 1. Location of the sampling stations during the IPY-CFL study, May to July 2008. Water depth is in meters. D: first-year drifting sea-ice stations; F: first-year landfast ice stations

the vertical stratification of the water column ($\Delta\sigma_t$, kg m^{-3}) was estimated as the difference in σ_t between 80 and 10 m from 1 May to 24 June and between 80 and 5 m after 24 June. At stations where bottom depth was <80 m, the deepest depth was used for the calculation. The mean irradiance in the surface mixed layer (E_{zm}, µmol photons m^{-2} s^{-1}) was calculated as per Riley (1957):

$$E_{zm} = \frac{E_0(1-e^{-K_d Z})}{K_d Z} \quad (2)$$

where Z is the depth of Z_m (m).

Water samples were generally collected within the surface mixed layer, which ranged from 4 to 44 m (Table 1). At IC stations, samples were collected in the upper 5 m of the water column through a hole in the sea ice made ~500 m from the ship, using a Kemmerer water sampler. Samples collected at depths >5 m were taken via the ship's moonpool with the CTD-rosette system. At OW stations, samples from the upper 5 m of the water column were collected with an electric submersible pump (12 V standard engineered plastic pump, model Cyclone, Proactive Environmental Products), whereas samples at depths >5 m were taken with the moonpool's CTD-rosette system. After 25 June, samples were collected with the CTD-rosette system deployed from the ship's upper deck.

Nutrients

Nitrate plus nitrite (NO_3+NO_2), nitrite (NO_2), phosphate (PO_4) and silicic acid ($Si(OH)_4$) concentrations were measured immediately after sampling using an onboard Bran-Luebbe 3 Autoanalyzer (adapted from Grasshoff et al. 1999).

Cell viability

Cell viability was assessed as the proportion of living cells in the algal community (%LC). It was determined by applying a cell membrane permeability

Table 1. Physical and chemical characteristics of ice-covered and open-water stations in the Beaufort Sea during spring and summer 2008. Z_m: surface mixed layer depth; $\Delta\sigma_t$: stratification index; E_0: downwelling incident PAR; E_{zm}: mean irradiance in the surface mixed layer; E_z: PAR at the sample depth; NO_3: nitrate; $Si(OH)_4$: silicic acid; PO_4: phosphate; nd: not determined

Stn	Date (2008)	Bottom depth (m)	Z_m (m)	$\Delta\sigma_t$ (kg m^{-3})	E_0 (µmol m^{-2} s^{-1})	E_{zm} (µmol m^{-2} s^{-1})	Sample depth (m)	E_z (µmol m^{-2} s^{-1})	NO_3 (µmol l^{-1})	$Si(OH)_4$ (µmol l^{-1})	PO_4 (µmol l^{-1})
Ice-covered stations											
D43	1 May	457	57	0.56	148	1	10	2	3.50	8.93	1.00
F1	10 May	53	15	0.36	650	2	0	3	nd	nd	nd
F1							2		nd	nd	nd
F1							5		nd	nd	nd
F2	14 May	192	21	0.63	1023	4	5	6	nd	nd	nd
F2	16 May	183	31	0.57	874	2	0	7	9.54	20.85	1.56
F2							5	5	9.49	20.91	1.55
F2							10	3	9.71	21.54	1.61
F5	28 May	368	14	nd	742	28	0	45	<0.03	2.51	0.77
D46	30 May	289	32	0.53	618	3	0	6	2.04	6.72	0.97
D46							5	4	3.02	8.58	1.04
D46							10	3	3.79	10.35	1.15
D47	31 May	273	16	0.47	475	2	0	3	nd	nd	nd
D47							5	3	nd	nd	nd
D47							10	2	1.36	6.31	0.94
F6	2 Jun	71	12	0.87	1213	7	5	7	0.18	5.37	0.91
F6							12	2	1.88	6.93	1.02
F7	8 Jun	78	13	0.82	1270	7	0	11	nd	7.55	0.83
F7							5	7	nd	5.79	0.77
F7							12	4	nd	18.14	1.17
F7	9 Jun	78	11	0.85	175	1	0	2	nd	nd	nd
F7							5	1	nd	nd	nd
F7							10	1	nd	nd	nd
F7	11 Jun	80	nd	0.51	216	nd	0	11	0.49	3.26	nd
F7							5	7	0.45	nd	nd
F7							12	4	5.94	17.61	nd
F7	13 Jun	79	13	0.91	855	3	5	4	nd	nd	nd
F7							12	1	nd	nd	nd
FB01	14 Jun	98	11	1.25	678	2	5	1	1.13	8.66	0.87
FB03	15 Jun	105	12	1.17	1096	8	5	8	1.25	7.30	0.80
FB05	15 Jun	107	10	1.46	1624	3	0	4	0.91	9.92	0.79
FB05							5	3	0.40	6.60	0.82
F7	18 Jun	80	13	1.07	205	69	12	28	nd	3.54	0.65
F7	19 Jun	125	13	1.44	590	42	2	72	1.66	3.80	0.64
FB07	21 Jun	112	14	1.61	152	11	12	7	0.62	4.14	0.76
F7	24 Jun	88	6	1.63	1552	29	0	55	nd	nd	nd
F7							6	13	0.59	2.19	0.54
FB07	25 Jun	103	5	1.78	459	46	0	81	nd	nd	nd
FB07							6	17	0.96	5.91	0.71

Table 1 continued on next page

test, the cell digestion assay (CDA; Agustí & Sánchez 2002), recently extended for quantification of dead phytoplankton cells in cold waters (Llabrés & Agustí 2008, 2010). In the CDA, phytoplankton communities are exposed to an enzymatic cocktail (DNAse and Trypsin) that enters the cytoplasm and digests cells with compromised membranes. The enzymes remove the dead or dying cells from the sample, and therefore the cells remaining in the samples after the CDA are considered living cells. For quantification of nano- and microphytoplankton viability, samples were concentrated from an initial volume of 0.3–2 l to 50–70 ml, using a device similar to the Millipore cell concentrator chamber used in previous studies (Agustí & Sánchez 2002, Alonso-Laita & Agustí 2006, Lasternas & Agustí 2010) fitted with a 2 µm pore diameter filter with a maximum time of concentration of 15 min. The CDA was applied (<2 min after concentration) to duplicate 10 ml aliquots of the cell concentrate by adding 2 ml of DNAse I solution (400 µg ml^{-1} in Hanks' balanced salt solution, HBSS), followed by 15 min incubation at 25°C in a water bath

Table 1 (continued)

Stn	Date (2008)	Bottom depth (m)	Z_m (m)	$\Delta\sigma_t$ (kg m^{-3})	E_0 (µmol m^{-2} s^{-1})	E_{zm} (µmol m^{-2} s^{-1})	Sample depth (m)	E_z (µmol m^{-2} s^{-1})	NO_3 (µmol l^{-1})	$Si(OH)_4$ (µmol l^{-1})	PO_4 (µmol l^{-1})
Open-water stations											
1020 A	6 May	276	42	0.6	1226	252	0	1226	4.83	9.78	1.17
1020 A							5	690	4.83	9.78	1.17
O2	12 May	205	21	0.67	178	67	0	178	nd	nd	nd
O2							2	142	nd	nd	nd
O2							5	100	9.45	20.47	1.56
O2							11	50	9.59	21.2	1.35
405b	19 May	537	17	0.68	1508	495	0	1508	nd	nd	<0.02
405b							5	648	nd	nd	1.11
405b							11	235	0.95	nd	0.92
1011	22 May	459	13	0.62	476	280	0	476	2.66	7.99	nd
1011							8	232	2.67	8.04	nd
1806	23 May	137	12	2.25	809	515	0	809	nd	nd	nd
1806							10	356	<0.03	2.63	0.75
9008	27 May	346	20	1.27	945	380	0	945	nd	nd	nd
9008							5	543	<0.03	3.03	0.8
405b	10 Jun	562	15	2.03	1544	739	7	695	nd	nd	nd
1216	23 Jun	207	9	3.1	1363	1363	0	1363	nd	nd	nd
1200	27 Jun	199	8	2.53	1250	852	0	1250	nd	nd	nd
1200							7	608	0.4	4.53	0.73
1208	28 Jun	400	6	1.81	181	135	7	88	<0.03	nd	0.77
434	30 Jun	40	4	2.13	270	205	5	132	nd	2.48	0.15
434							13	42	nd	1.91	0.36
421	1 Jul	1142	8	4.90	223	166	9	110	<0.03	3.71	0.31
420	9 Jul	43	6	1.88	316	238	7	158	<0.03	4.77	0.35
1100	11 Jul	265	6	3.15	1044	800	7	545	0.66	4.78	nd
1110	12 Jul	96	4	2.15	35	27	7	14	<0.03	3.27	<0.02
D34	13 Jul	182	4	4.27	1384	1176	10	599	<0.03	4.28	0.70

(Haake). After this time, 2 ml of Trypsin solution (1% in HBSS) was added, followed by 30 min at 25°C. Additional duplicate 10 ml aliquots from the concentrate without enzymes were incubated to obtain the blanks for each sample analyzed. After incubation, samples with enzyme additions were then placed in ice to stop the enzymatic cell digestion process and then both blanks and samples containing enzymes were filtered onto polycarbonate 0.4 µm pore diameter black filters, washed several times with filtered seawater, fixed with glutaraldehyde (1% final concentration) and stored frozen at −80°C until microscopic counts. Phytoplankton cells were observed until ≥200 cells had been counted at magnifications of 400× and 1000× using an epifluorescence microscope (Zeiss Axiovert©) fitted with a blue excitation red fluorescence filter. Cells were grouped by size into 3 groups: >20, 5–20 and <5 µm.

The cell counts in the samples after the CDA assay represent the abundance of living cells. The cell abundance in the blank samples represents the total cell abundance, i.e. both living and dead cells (Agustí & Sánchez 2002). The %LC was calculated as the ratio of the concentration of cells obtained after applying the CDA to the concentration of cells in the blanks.

The accuracy of the CDA to quantify living and dead cells in polar natural samples was tested by comparing the results obtained with the CDA with those obtained with an independent vital stain, the BacLight™ kit (Molecular Probes® Fluorescent Dyes and Probes, Invitrogen). This method was chosen among others because it uses double staining (SYTO 9 and propidium iodide), avoiding the potential ambiguity of other stains with low fluorescence signals (e.g. fluorescein diacetate; Agustí & Sánchez 2002, Garvey et al. 2007, Llabrés & Agustí 2008). The BacLight™ is a vital stain that works well with diatoms (a major component of the ice algae community; Rózanska et al. 2009). With this method, diatoms show a clear and bright staining (Llabrés & Agustí 2008).

The 2 methods, CDA and BacLight™, were compared during an experiment conducted onboard the

CCGS 'Amundsen' during the IPY-CFL system study (Alou-Font 2013). This experiment was performed to test the effect of prolonged darkness and high temperature on cell viability. Cells collected at the bottom of the sea-ice on 29 April were incubated in the dark at room temperature (15–20°C) for 10 d. Algal cell viability was determined with both methods after 3 d of acclimation on 2, 5 and 9 May.

For the BacLight™ method, duplicate 1 ml samples were stained with 0.2 µl of BacLight™ kit component B: SYTO 9 dye (1.67 mM) and propidium iodide (1.83 mM) both in dimethyl sulfoxide, and incubated for 10 to 15 min in the dark following the same procedure as in Agustí et al. (2006) and Llabrés & Agustí (2008). Quantitative analysis was conducted on board the ship with an Olympus epifluorescence microscope fitted with a blue filter (excitation 470 nm, emission 520–560 nm). In total, 200 cells were counted, distinguishing green cells (living cells), red cells (dead cells) and not well-stained cells. The percentage of living cells was calculated as the ratio of red cells to total cell abundance.

Taxonomic analysis

Eleven subsamples on which viability was assessed were selected for a detailed taxonomic analysis. These samples were preserved with acidic Lugol's solution (0.4% final concentration) and stored in the dark at 4°C until analysis. Living cells (with chloroplasts) >2 µm were identified by an experienced phytoplankton taxonomist (S. Lessard pers. comm.) using an inverted light microscope (WILD Heerbrugg). A minimum of 400 cells were enumerated over at least 3 transects of the chamber (Lund et al. 1958).

Index of photosynthetic performance (F_v/F_m)

The photosynthetic performance of algae from the surface layer (0–15 m) was assessed by examining the changes in chlorophyll fluorescence with the electron transport inhibitor 3-(3,4-dichlorophenyl)-1,1-dimethylurea (DCMU) that blocks electron transport at the electron acceptor Q in PSII, causing an increase in chlorophyll fluorescence (Roy & Legendre 1979, Jochem 2000). Minimum and maximum fluorescence (F_0, F_m) were measured after 30 min of dark adaptation using a Turner Designs 10-AU fluorometer. F_m was measured after adding DCMU (3×10^{-3} M). F_v/F_m was calculated as $(F_m - F_0)/F_m$, providing an index of photosynthetic performance. A decrease in the maximum quantum yield of PSII photochemistry, measured as dark-adapted F_v/F_m in the presence of DCMU, is a proxy for photoinhibition or down-regulation of PSII (Critchley 2000).

Pigment analysis

The identity and concentrations of algal pigments were determined by reverse-phase high performance liquid chromatography (HPLC). Under dim light, water samples (0.25–2 l) were filtered onto 25 mm Whatman GF/F filters (maximum time of filtration of 20 min). The samples were immediately placed in liquid nitrogen for at least 24 h and then transferred to a −80°C freezer on board the ship. Samples were sent every 6 wk by plane in a nitrogen dry-shipper and thereafter kept in a −80°C freezer until analysis. Algal pigments were extracted in 95% methanol, sonicated (Sonicator Ultrasonic Processor XL 2010) for 15 s on ice and centrifuged for 5 min at 3700 × *g*. Extracts were filtered through a 0.22 µm polytetrafluoroethylene syringe filter and poured into an autosampler vial which was gently sparged with argon to limit oxidation. A volume of 50 µl was injected in a Waters Symmetry C_8 column (150 × 4.6 mm, 3.5 µm). Gradient elution was controlled by a Thermo Separation (TSP) P4000 pump with solvents as described by Zapata et al. (2000). Pigments were detected with a TSP UV6000 LP diode-array absorbance detector (400 to 700 nm) and a TSP FL3000 fluorescence detector to confirm the presence of chlorophyll-related compounds. Calibration was done with external pigment standards (DHI Lab Products), and extinction coefficients were taken from Jeffrey (1997). Limits of detection and quantification were estimated as in Bidigare et al. (2005) and pigments with concentrations less than the limit of detection are not reported in the present study. Marker pigments were identified through comparison with the retention time and spectral properties of pigment standards (Egeland et al. 2011).

Statistical analyses

Spearman's rank order correlations (r_S) were used to determine any significant correlations among physical, chemical and biological variables. A Mann-Whitney *U*-test was performed to seek differences among IC and OW stations, whereas a Kruskal-Wallis test was used to seek differences between

binned data for 5 irradiance intervals and for 3 temperature intervals. Descriptive statistics, r_S, and Pearson's linear regressions were obtained using SigmaStat 3.5 and SigmaPlot 10.0 (Systat Software). Unless otherwise noted, all mean values are ±SE.

RESULTS

Physico-chemical variables

The seasonal increase in daily incident PAR ranged from 23.6 mol photons m^{-2} on 17 May (Stn F2) to 66.1 mol photons m^{-2} on 20 June (Stn F7; Fig. 2a). Irradiance in the surface layer was influenced by ice cover: it differed significantly between the 2 sets of stations, viz. IC and OW. The percent sea-ice cover ranged from 20 to 95% in May, decreasing to 10% in June and reaching a minimum in July (<5%) (Forest et al. 2011). We present results separately for both sets of stations.

The PAR at the sampling depth (E_z) and the mean irradiance in the surface mixed layer (E_{zm}) were significantly higher (Mann-Whitney *U*-test, $p < 0.001$) for OW (418.7 ± 82.6 and 364.6 ± 62.1 µmol photons m^{-2} s^{-1}, respectively) than for IC stations (7.4 ± 2.0 and 10.9 ± 2.7 µmol photons m^{-2} s^{-1}, respectively; Table 1).

Water temperatures for the surface layer during the study period were significantly higher (Mann-Whitney *U*-test, $p < 0.05$) in OW (2.57 ± 0.94°C) compared to IC stations (–0.63 ± 0.33°C). Water temperatures increased throughout the sampling period and reached maximum values at the end of the study on 11 July (8°C, Stn 1100) and 13 July (7°C, Stn D34; Figs. 1 & 2b). Salinity values ranged from 27 to 33 with values of 30.56 ± 0.42 at OW and 31.91 ± 0.18 at IC stations. Lower salinity was measured at Stns 421 and D34 at the end of the study (Fig. 2b). The stratification index ($\Delta\sigma_t$) ranged from 0.60 to 4.90 kg m^{-3} for OW (1.67 ± 0.25 kg m^{-3}) and from 0.36 to 1.78 for IC (0.88 ± 0.07 kg m^{-3}). Significant differences were found for salinity and $\Delta\sigma_t$ between the OW and IC stations, with salinity being significantly higher at IC stations (Mann-Whitney *U*-test, $p < 0.01$) and $\Delta\sigma_t$ significantly higher at OW stations (Mann-Whitney *U*-test, $p < 0.01$) and increasing throughout the season (see Table 1). The surface mixed layer (Z_m) averaged 14.58 ± 1.82 m throughout the study period and did not differ significantly between the OW and IC stations (Mann-Whitney *U*-test, $p > 0.05$; Table 1).

Nutrient concentrations (in µmol l^{-1}) in the surface layer varied over the entire study: for NO_3, values ranged from <0.03 to 9.6 (OW = 2.2 ± 0.9, IC = 2.7 ± 0.6), for $Si(OH)_4$, from 1.9 to 21.5 (OW = 6.8 ± 1.6, IC = 9.2 ± 1.2) and for PO_4, from <0.02 to 1.60 (OW = 0.73 ± 0.12, IC = 0.96 ± 0.06). There were no significant differences between OW and IC stations (Mann-Whitney *U*-test, $p = 0.13$ for NO_3; $p = 0.07$ for PO_4 and $Si(OH)_4$). The NO_3:PO_4 and NO_3:$Si(OH)_4$ molar ratios decreased over the study and were lower than the critical values of 16 for NO_3:PO_4 (Redfield et al. 1963) and of 1.1 for NO_3: $Si(OH)_4$ (Brzezinski 1985), suggesting that nitrogen was the potentially limiting nutrient for algal growth.

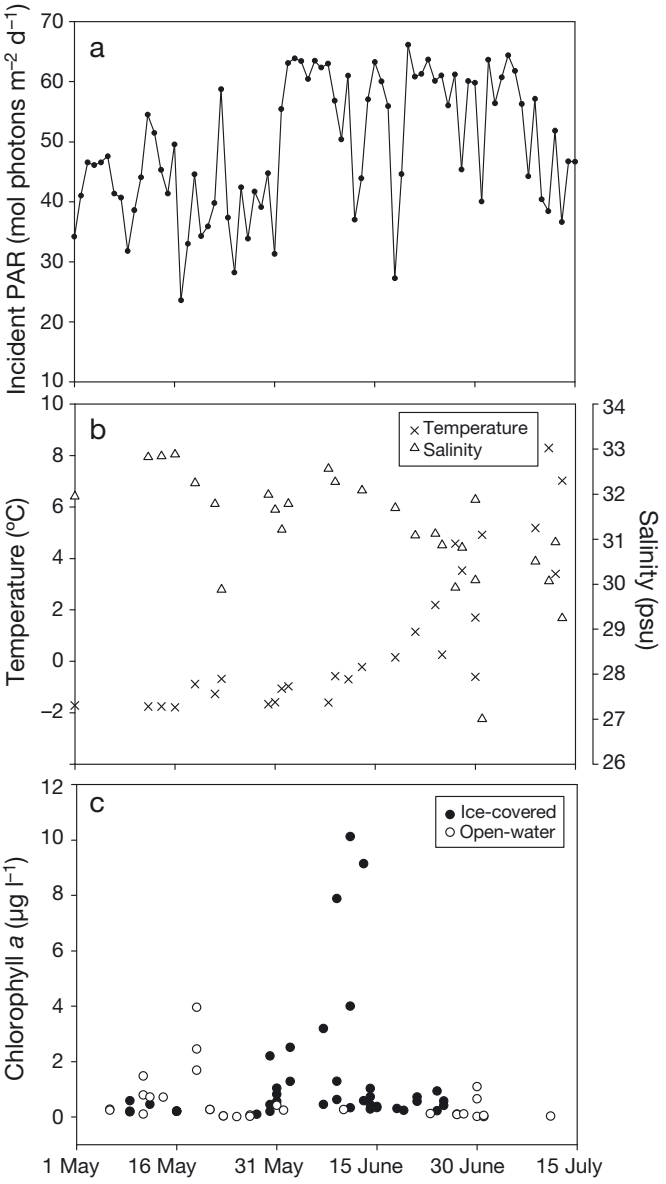

Fig. 2. Temporal changes in (a) daily incident irradiance, (b) surface layer water temperature and salinity, and (c) surface layer chlorophyll *a* concentration at ice-covered and open-water stations from May to July 2008

Algal biomass

The surface layer chl *a* concentration was significantly lower (Mann-Whitney *U*-test, $p < 0.05$) at OW (0.67 ± 0.22 µg l^{-1}) than at IC stations (1.50 ± 0.41 µg l^{-1}; Fig. 2c). The algal biomass reached a maximum for OW stations on 19 May (3.95 µg l^{-1}, Stn 405b, 0 m) and for IC stations on 11 June (10.13 µg l^{-1}, Stn F7, 5 m), the peak of the observed bloom. Wind-driven upwelling events enhanced under-ice nutrient availability (Mundy et al. 2009, Tremblay et al. 2011), causing the high chl *a* concentrations encountered during this study at IC stations in Darnley Bay (Fig. 2c). After this period, chl *a* concentrations decreased to 0.01 µg l^{-1} at OW stations. The low chl *a* values encountered at the end of the study co-occurred with the lowest nutrient concentrations, suggesting nutrient-depleted post-bloom conditions. There was no significant relationship between chl *a* concentration and any of the nutrients determined at IC stations, whereas at OW stations, chl *a* was positively correlated with NO_3 ($r_S = 0.76$, $p < 0.01$) and $Si(OH)_4$ ($r_S = 0.68$, $p < 0.05$).

The chl *a* concentration did not show any significant relationship with daily incident irradiance, water temperature and salinity at OW and IC stations, but it was negatively correlated with $\Delta\sigma_t$ for OW stations ($r_S = -0.68$, $p < 0.05$).

Table 2. Main marker pigments, photoprotective pigments, and degradation pigments measured at ice-covered (IC) and open-water (OW) stations. Hex-fuco: 19′-hexanoyloxyfucoxanthin; but-fuco: 19′-butanoyloxyfucoxanthin; PPC: photoprotective carotenoids; PSC: photosynthetic carotenoids (see 'Results' for details of pigments in each group); DD+DT: sum of diadinoxanthin and diatoxanthin. Mean values ± SE are shown; n = number of samples; p values are given for significant differences between IC and OW stations; ns: no significant difference. All concentrations are given in µg l^{-1}; all ratios are wt:wt

Concentration and ratio	IC stations Mean ± SE	n	OW stations Mean ± SE	n	p
Marker pigments					
Chlorophyll *b* (chl *b*)	0.17 ± 0.02	39	0.05 ± 0.01	28	<0.01
Peridinin (Peri)	0.04 ± 0.004	29	0.03 ± 0.004	15	ns
Fucoxanthin (Fuco)	0.48 ± 0.16	40	0.18 ± 0.06	30	<0.01
Alloxanthin (Allo)	0.01 ± 0.001	25	0.01 ± 0.000	13	ns
Prasinoxanthin (Prasino)	0.01 ± 0.001	25	0.002 ± 0.02	13	<0.01
Hex-fuco	0.02 ± 0.002	21	0.02 ± 0.01	18	ns
But-fuco	0.01 ± 0.002	28	0.01 ± 0.002	11	ns
Micromonal (Micral)	0.02 ± 0.002	20	0.01 ± 0.000	7	<0.01
Zeaxanthin (Zea)	0.02 ± 0.001	33	0.01 ± 0.000	23	<0.05
Chl *b*:chl *a*	0.24 ± 0.03	29	0.25 ± 0.04	30	ns
Peri:chl *a*	0.07 ± 0.01	29	0.08 ± 0.02	16	ns
Fuco:chl *a*	0.26 ± 0.02	30	0.35 ± 0.07	32	ns
Allo:chl *a*	0.02 ± 0.002	25	0.03 ± 0.01	13	ns
Prasino:chl *a*	0.05 ± 0.03	37	0.09 ± 0.02	25	ns
Hex-fuco:chl *a*	0.03 ± 0.003	22	0.05 ± 0.01	17	ns
But-fuco:chl *a*	0.02 ± 0.002	28	0.03 ± 0.003	11	ns
Micral:chl *a*	0.03 ± 0.004	20	0.03 ± 0.004	8	ns
Zea:chl *a*	0.03 ± 0.003	27	0.14 ± 0.06	25	<0.05
Chl *a* and photoprotective pigments					
Chl *a*	1.50 ± 0.41	36	0.67 ± 1.02	20	<0.05
PPC	0.12 ± 0.02	36	0.07 ± 0.02	18	<0.05
PSC	0.62 ± 0.18	36	0.25 ± 0.09	20	<0.01
PPC:PSC	0.36 ± 0.03	36	0.53 ± 0.14	18	ns
PPC:chl *a*	0.14 ± 0.06	30	0.24 ± 0.05	18	<0.05
(DD+DT):chl *a*	0.07 ± 0.01	36	0.15 ± 0.03	18	<0.01
Degradation pigments					
Chl *a* allomer	0.22 ± 0.09	27	0.10 ± 0.03	10	ns
Chlorophyllide *a*	0.22 ± 0.07	23	0.20 ± 0.08	11	ns
Pheophorbide *a*	0.41 ± 0.12	37	0.18 ± 0.28	19	<0.05
Pheophytin *a*	0.25 ± 0.07	12	0.14 ± 0.06	4	ns
Pyropheophorbide *a*-'like'	0.65 ± 0.08	19	0.30 ± 0.03	5	<0.05
Sum of all degradation pigments	1.1 ± 0.30	37	0.43 ± 0.14	19	ns
Chl *a* allomer:chl *a*	0.08 ± 0.05	27	0.13 ± 0.03	10	ns
Chlorophyllide *a*:chl *a*	0.09 ± 0.05	23	0.12 ± 0.03	11	ns
Pheophorbide *a*:chl *a*	0.26 ± 0.09	36	0.33 ± 0.07	19	ns
Pheophytin *a*:chl *a*	0.07 ± 0.03	11	0.18 ± 0.09	4	ns
Pyropheophorbide *a*-'like':chl *a*	0.86 ± 0.66	19	1.90 ± 1.4	5	ns
Sum of all degradation pigments:chl *a*	0.88 ± 0.63	36	1.70 ± 0.38	19	ns

Pigment markers for taxonomic groups

The major marker pigments detected were used to assess the composition of phytoplankton groups (Higgins et al. 2011) along with the microscopic examination (few data) and past observations from this polar region (Lovejoy et al. 2007, Poulin et al. 2011). These marker pigments are listed in Table 2; they include fucoxanthin for diatoms (fucoxanthin is also present in a few other groups, but diatoms were clearly dominant so we used this pigment as a marker for diatoms here), prasinoxanthin for prasinoxanthin-containing prasinophytes, peridinin for peridinin-containing dinoflagellates, alloxanthin for cryptophytes, and 19′-hexanoyloxyfucoxanthin (hex-fuco) and 19′-butanoyloxyfucoxanthin (but-fuco) for haptophytes. Chl *b*, micromonal and zeaxanthin were also present and strongly correlated with prasinoxanthin (r_S = 0.74, 0.86 and 0.92,

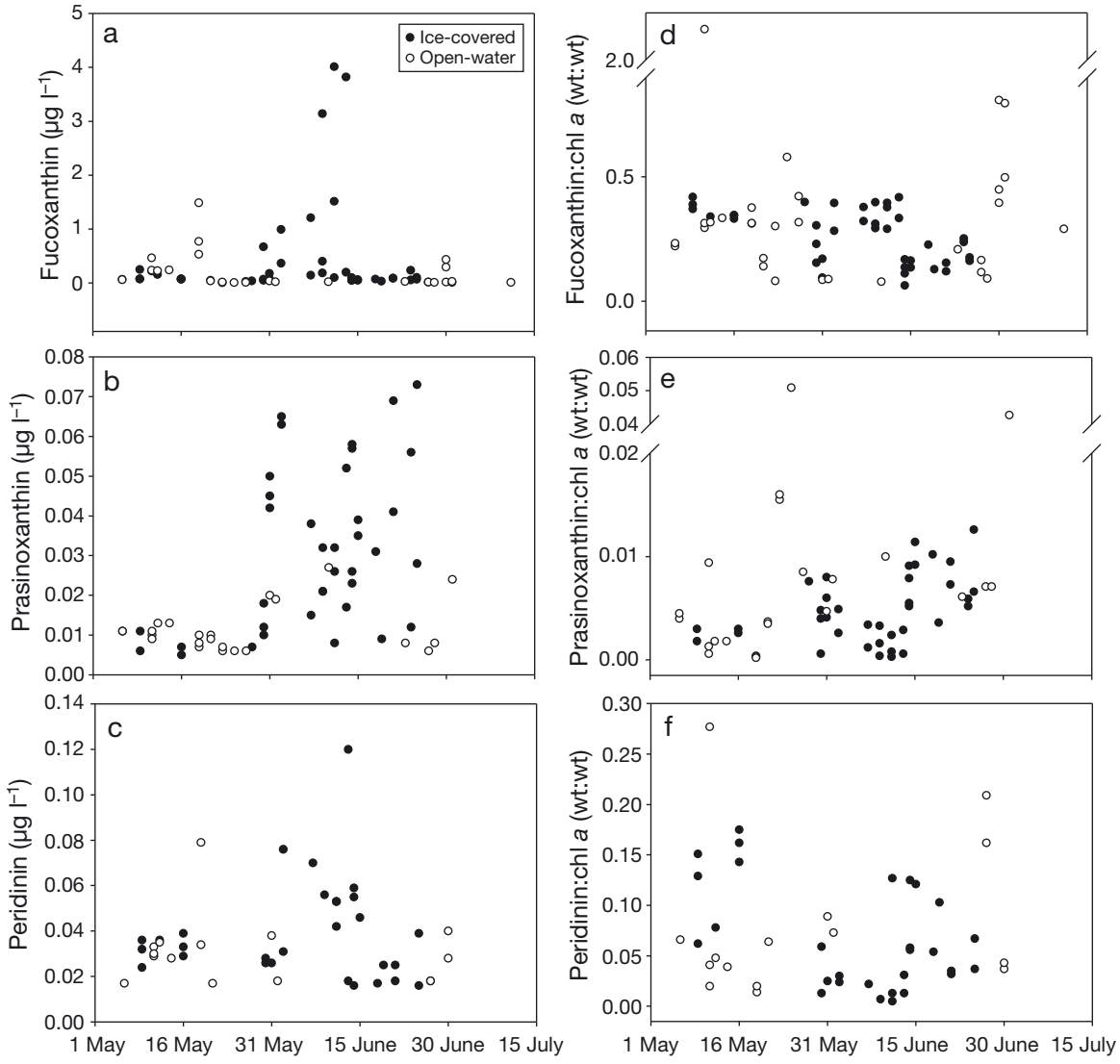

Fig. 3. Temporal changes in the concentrations of (a) fucoxanthin, (b) prasinoxanthin, and (c) peridinin and in the ratios of (d) fucoxanthin, (e) prasinoxanthin, and (f) peridinin to chlorophyll *a* at ice-covered and open-water stations from May to July 2008

respectively), suggesting that they belonged to the prasinophytes. Complete analysis of the pigment data set is outside of the scope of this work, but the relative importance of these algal groups can be obtained by dividing the mean concentration of these marker pigments for the 2 groups of stations (OW and IC) by the mean field-derived marker pigment: chl *a* ratio for the respective algal groups (from Higgins et al. 2011, using low-light ratios for IC stations). Results show that overall, for both sets of stations, diatoms and prasinophytes are the 2 algal groups with the greatest contribution to total chl *a* biomass (mean values for diatoms: 40% for OW stations, 30% for IC stations; prasinophytes: 35% for OW stations, 20% for IC stations), followed by cryptophytes and dinoflagellates (roughly 10% for both sets of stations) and haptophytes (roughly 5%). Microscopic observations match relatively well with pigment-based community composition, with the presence of centric diatoms (e.g. the genera *Chaetoceros* and *Thalassiosira*) and pennate diatoms (e.g. *Fragilariopsis* spp., *Fossula* spp., *Nitzschia* spp. and *Cylindrotheca* spp.), dinoflagellates (e.g. *Gymnodinium* spp., *Gyrodinium* spp.), prasinophytes (e.g. *Pyramimonas* spp.) and cryptophytes (e.g. *Plagioselmis* spp.), and finally unidentified flagellates.

Temporal patterns for these various algal groups obtained based on pigment composition are shown in Fig. 3. Diatoms (expressed as fucoxanthin concentration and the fucoxanthin:chl *a* ratio, Fig. 3a,d) were

present throughout the study period at both OW and IC stations, representing nearly a third of the total chl *a*. The temporal distribution of fucoxanthin displayed the same trend as chl *a*. For IC stations, maximum concentrations were observed on 9 to 13 June, while for OW stations, concentrations were lower, with a first maximum around 19 May and a second smaller maximum in late June. The fucoxanthin:chl *a* ratio was around 0.3, slightly higher for OW stations particularly after the bloom in early June. Prasinophytes (Fig. 3b,e) represented less than 30% of total chl *a* and showed different trends for the 2 groups of stations: for OW stations, maximum concentrations of prasinoxanthin were seen in May (Stn 405), around 10 June (Stn 405b) and at the end of June (Stn 421), whereas for IC stations there was an increase over time, both in terms of concentration of prasinoxanthin and of the prasinoxanthin:chl *a* ratio. Dinoflagellates (Fig. 3c,f) were also present throughout the study, at roughly 10% of the total chl *a*, with a pattern that resembled fucoxanthin-containing diatoms.

Photoprotective pigments

The ratio of photoprotective carotenoids (PPC; sum of diadinoxanthin [DD], diatoxanthin [DT], violaxanthin, zeaxanthin, lutein and β,β-carotene) to photosynthetic carotenoids (PSC; sum of fucoxanthin, peridinin, neoxanthin, alloxanthin, prasinoxanthin, hex-fuco and but-fuco) increased seasonally (data not shown). This increase was greater for OW stations (PPC:PSC, 0.16–2.52 wt:wt) than for IC stations (0.09–0.77 wt:wt, Table 2). A similar trend was seen for the PPC:chl *a* ratio (not shown), which ranged from about 0.07 to 0.60 (wt:wt) at OW stations and 0.04 to 0.26 (wt:wt) at IC stations. The increase of the PPC concentration was mostly due to DD (33% of PPC), β,β-carotene (20%) and violaxanthin (14%). The ratios indicating the relative importance of photoprotective pigments, such as PPC:chl *a* and (DD+DT):chl *a* ratios, were significantly higher at OW stations (see Table 2), suggesting that the most abundant taxonomic group, viz. diatoms (which contain fucoxanthin, DD and DT), increased photoprotection through the xanthophyll cycle in OW stations in response to the higher irradiances of OW stations.

Validation of the CDA viability method

The CDA viability method was validated against the vital stain BacLight™. Both methods showed similar results (Table 3). The percentage of living cells of *Nitzschia frigida* decreased from 86.3 ± 4.9% on 2 May to 14.2 ± 1.4% at the end of the experiment on 9 May. The viability obtained with the BacLight™ method showed a similar trend with time. Mann-Whitney *U*-tests revealed no significant differences in the percentage of living cells of *N. frigida* between the CDA and the BacLight™ methods when sampled on 2 May ($p = 0.35$), 5 May ($p = 0.35$) and 9 May ($p = 0.06$), from the dark and room temperature test (Table 3). These results on *N. frigida* validate the use of the CDA assay when used for Arctic species.

Table 3. Percent living cells of *Nitzschia frigida* (mean ± SE) estimated using the enzymatic cell digestion assay (CDA) and the BacLight™ viability kit. Number of observations: n = 4 for CDA; n = 2 for the BacLight™ kit

Method	2 May	5 May	9 May
CDA	86.3 ± 4.9	22.7 ± 7.1	14.2 ± 1.4
BacLight™ kit	91.5 ± 0.8	15.7 ± 1.3	10.0 ± 3.0

Variability of living cells

For both sets of stations, the %LC for the total community was most strongly correlated with the abundance of the 5–20 µm cells ($r_S = 0.90$, $p < 0.001$), followed by cells >20 µm ($r_S = 0.78$, $p < 0.001$) and <5 µm ($r_S = 0.60$, $p < 0.001$). Overall, the ranges of %LC values were large and there were no significant differences between OW and IC stations ($p > 0.05$, 57.3 ± 5.8% and 48.0 ± 3.9%, respectively). The cell abundance ranged from 1.38×10^3 cells l^{-1} at Stn D34 to 4.56×10^6 cells l^{-1} at Stn D43.

In general, there was a match between high algal biomass and high %LC, in the bloom periods of mid-May for OW and beginning of June for IC sites. At OW after the period of maximum chl *a* in May and the smaller maximum in late June, there was no clear decrease in %LC, while at IC, there was a sharp decrease in %LC following the demise of the bloom. The %LC at both sets of stations varied widely with environmental variables throughout the study, and did not show a significant relationship with nitrate concentration (not shown). However, we note that the lowest %LC values (<20%) encountered at low nitrate concentrations (<0.2 µmol l^{-1}) are characterized by a greater abundance of prasinophytes relative to diatoms.

The relationship between %LC and *in situ* irradiance (E_z) was different between OW and IC stations.

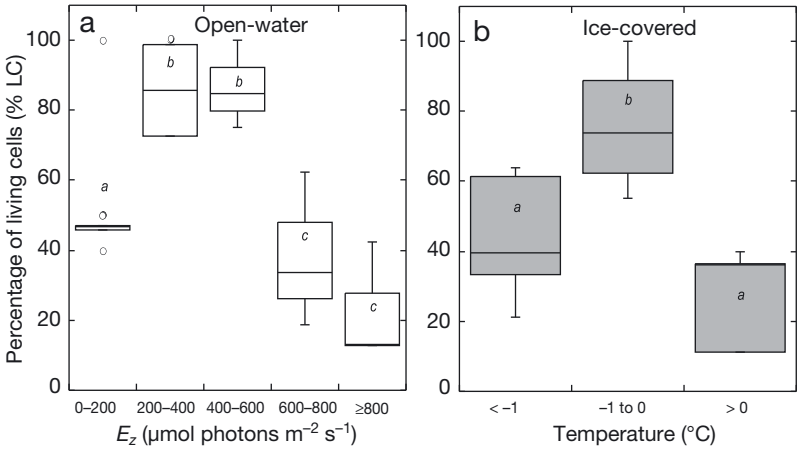

Fig. 4. Relationship between (a) percentage of living cells (%LC) and PAR at sampling depth (E_z) at open-water stations. The data were binned for 5 irradiance intervals (i.e. 0–200, n = 5; 200–400, n = 3; 400–600, n = 3; 600–800, n = 3; and ≥800 µmol photons m^{-2} s^{-1}, n = 3). (b) %LC and water temperature at ice-covered stations. The data were binned for 3 temperature intervals (i.e. < −1, n = 6; −1 to 0, n = 4; and >0, n = 6). Boxes represent the lower and upper quartiles, median, minimum and maximum values, and outliers. Boxes with the same lowercase letters in *italics* are not significantly different ($p < 0.05$)

At OW stations, the %LC maximum values (86.7 ± 7.2%) were found at irradiances between 200 and 600 µmol photons m^{-2} s^{-1} (Fig. 4a). There was a clear decrease in %LC as irradiances increased throughout the season: lowest %LC values (22.7 ± 9.8%) were found at irradiances ≥600 µmol photons m^{-2} s^{-1} (Fig. 4a). These %LC values were significantly lower than the averaged %LC values found at irradiances between 200 and 600 µmol photons m^{-2} s^{-1} (Kruskal-Wallis test, $p < 0.05$, 86.6 ± 7.2%, see Fig. 4a). After the second smaller biomass maximum (30 June to 15 July), the phytoplankton community of the OW stations showed an increase of %LC over time, matching with a decrease of the incident PAR during this period (see Fig. 2a). At OW stations with >50% LC (n = 5) and E_z <200 µmol photons m^{-2} s^{-1}, diatoms, prasinophytes and other groups of flagellated cells made up 40, 6 and 30% of the total chl *a* biomass, respectively. For stations with <50% LC and E_z <200 µmol photons m^{-2} s^{-1} (n = 5), the dominant algal groups were diatoms (26%), prasinophytes (26%) and cryptophytes (23%). Finally, for samples with low %LC and high irradiances (>600 µmol photons m^{-2} s^{-1}), diatoms (39%), cryptophytes (8%) and prasinophytes (7%) dominated. Hence at OW stations, high %LC were seen only at moderate irradiances (<600 µmol photons m^{-2} s^{-1}) and were dominated by diatoms, but a large proportion of these cells died when irradiances increased above this threshold.

For IC stations, %LC varied widely with E_z and did not show a significant relationship (r_S = 0.09, p = 0.61). The %LC ranged from 6 to 100% (mean ± SE: 49.7 ± 4.5%) at irradiances <15 µmol photons m^{-2} s^{-1} and from 18 to 59% (38.8 ± 5.4%) at irradiances >15 µmol photons m^{-2} s^{-1}. We examined whether the changes in algal community could explain the high variability of the %LC for E_z <15 µmol photons m^{-2} s^{-1} by comparing the pigment composition of samples having %LC >75% and samples with %LC <25% (n = 6). The stations with >75% LC had, on average, 39% diatoms, 5% prasinophytes and minor contributions from a few other groups to the total chl *a*. Stations with <25% LC presented a higher contribution of prasinophytes (21%), followed by diatoms (18%) and cryptophytes (8%). Stations with E_z values >15 µmol photons m^{-2} s^{-1} (maximum of 60 µmol photons m^{-2} s^{-1}) were mainly composed of prasinophytes (33%) followed by diatoms (22%) and other groups (<5%).

The relationship between %LC and water temperature differed between OW and IC stations, with a clear decrease of %LC at temperatures above 0°C for IC stations (Fig. 4b). The %LC of IC stations was significantly higher between −1 and 0°C (Kruskal-Wallis test, $p < 0.05$, 79.3 ± 7.2%) than at < −1°C (43.2 ± 6.8%) or at higher temperatures >0°C (30.9 ± 6.6%, see Fig. 4b). The community was mainly composed of diatoms at temperatures <0°C (37% diatoms, 14% prasinophytes and <10% contribution from other groups, n = 10) and of prasinophytes at temperatures >0°C (33% prasinophytes, 19% diatoms and 10% cryptophytes, n = 3). At OW stations, %LC tended to increase above 0°C (data not shown), but did not show significant changes with water temperature. The phytoplankton community at these stations above 0°C was mainly composed of diatoms (45% diatoms and 34% prasinophytes, with <5% contribution from other groups, n = 4).

Living cells and photosynthetic performance

During the period of study, the total %LC was significantly correlated with F_v/F_m for all stations and depths (r_S = 0.34, $p < 0.05$, n = 53). This correlation was improved slightly when considering only IC stations (r_S = 0.36, $p < 0.05$, n = 33, Fig. 5a).

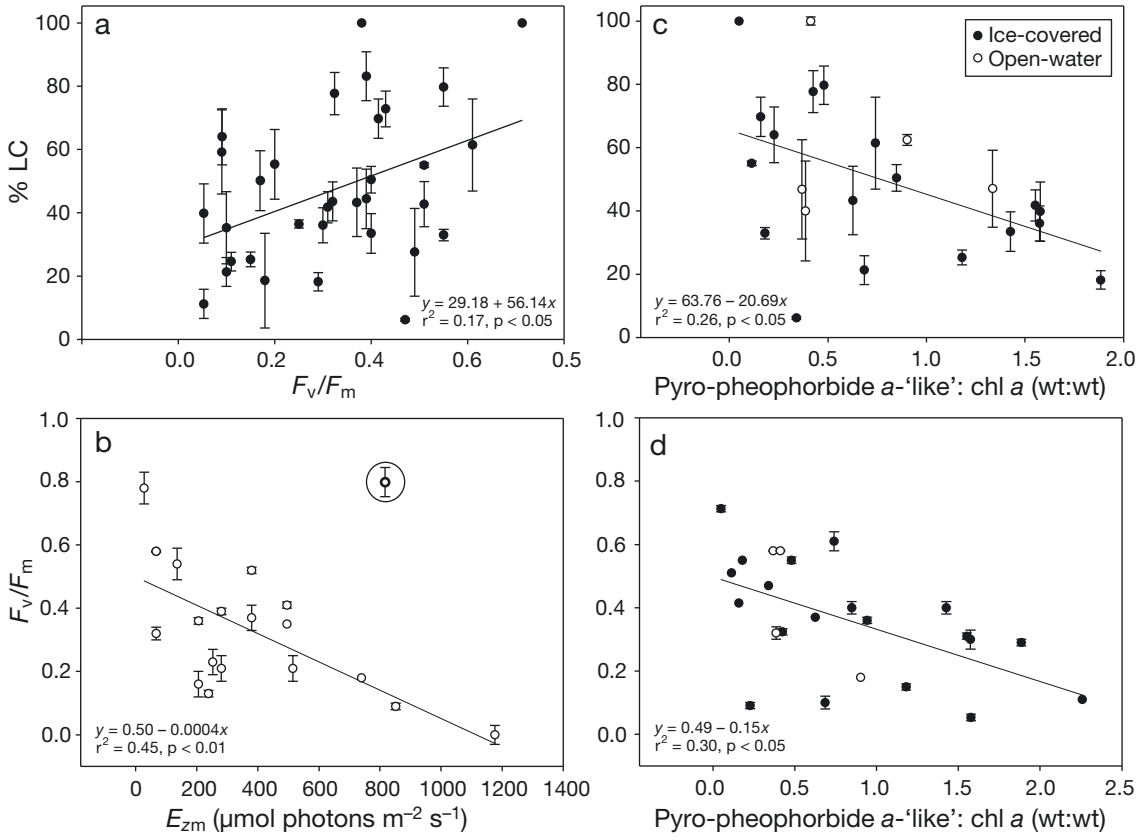

Fig. 5. Relationships between (a) percentage of total living cells (%LC) and photosynthetic performance (F_v/F_m), (b) F_v/F_m and mean PAR in the surface mixed layer (E_{zm}), (c) %LC and pyropheophorbide *a*-'like':chl *a* ratio, and (d) F_v/F_m and pyropheophorbide *a*-'like':chl *a* ratio at ice-covered and/or open-water stations. For %LC and F_v/F_m, mean values and SEs are presented. A model I regression line is shown for each graph. In (b), the circled value (outlier) was not used for computing the regression

The relationship between F_v/F_m and mean irradiance in the surface mixed layer (E_{zm}) differed between the 2 sets of stations. At OW stations, we observed a significant negative relationship between the F_v/F_m values and E_{zm} (Fig. 5b) when an outlier, Stn 1110 (799 µmol photons m^{-2} s^{-1}, $F_v/F_m = 0.8$, 75% LC), was omitted, suggesting that high irradiance had a negative influence on the photosynthetic performance of the cells in open waters. However, our results showed no significant relationship between these 2 variables at IC stations. For all stations, the F_v/F_m index was negatively correlated with $\Delta\sigma_t$ ($r_S = -0.31$, $p < 0.05$, $n = 53$). There were no other significant correlations between F_v/F_m and environmental variables.

Degradation pigments

We identified 6 chlorophyll degradation products: chl *a* allomer and epimer, chlorophyllide *a*, pheophorbide *a*, pheophytin *a*, and a pyropheophorbide *a*-'like' pigment (see Table 2 and Fig. 6 for the absorption spectrum of this pigment). The sum of chl *a* allomer and epimer generally made up <15% of chl *a*. The concentrations of pheophorbide *a* and pyropheophorbide *a*-'like' were significantly lower at OW than IC stations (Table 2), as was the concentration of chl *a*. When normalized to chl *a* (wt:wt), there were no differences in the concentration of any of the degradation pigments detected between both sets of stations.

The ratio of the pigment pyropheophorbide *a*-'like' to chl *a* (wt:wt) was significantly correlated with $\Delta\sigma_t$ at IC stations ($r_S = 0.49$, $p < 0.05$, $n = 20$). No other significant relationship was found between any of the degradation pigments (normalized to chl *a*) and other physico-chemical variables at IC stations ($p > 0.05$).

After the removal of 1 outlier (assumed to be an artifact due to the presence of fecal pellets), the pyropheophorbide *a*-'like' concentration (normalized to chl *a*) presented a significant negative relationship

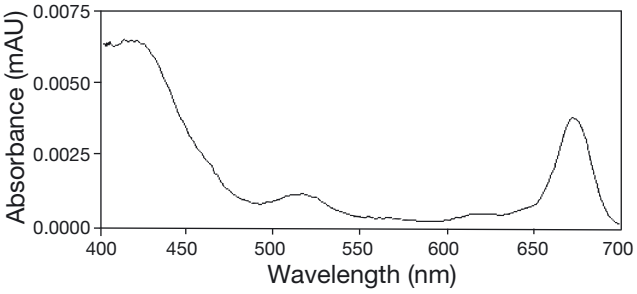

Fig. 6. Spectrum of the detected degradation pigment pyropheophorbide *a*-'like' in the HPLC solvent system of Zapata et al. (2000). mAU: milli-Absorbance Units

with the %LC and with F_v/F_m for OW and IC stations (Fig. 5c,d), suggesting that it could be used as a tracer of low cell viability conditions.

DISCUSSION

Water temperature and salinity values observed during this study (Fig. 2) were characteristic for the upper water layer in the area, the polar mixed layer, which is highly influenced by freezing–melting and river inputs (salinity < 33, temperature ~ −1.5°C, Carmack & Macdonald 2002). The spring–summer 2008 was characterized by an unusually low sea-ice cover and warm sea surface temperatures (Forest et al. 2011). As the season progressed, the surface temperatures increased, reaching the observed maximum values, coinciding with the complete retreat of the sea-ice cover by the end of the study. Surface salinity was lowered due to the summer sea-ice melting that increased stratification and reduced the depth of the surface mixed layer (Tremblay et al. 2012). The distribution of nutrients and phytoplankton biomass during the study period have been discussed elsewhere (Mundy et al. 2009, Brown et al. 2011, Tremblay et al. 2011); 3 consecutive wind-driven upwelling events enhanced the under-ice nutrient availability leading to the observed peaks in chl *a* concentrations at IC stations (Fig. 2c). Lower surface layer nutrient concentrations were observed at OW stations (Table 1), likely because of high stratification, especially later in the season, reducing nutrient replenishment. Vertical stratification and nutrient availability are thought to drive the structure and shape of phytoplankton communities of the surface waters in the Beaufort Sea (Hill et al. 2005). The Arctic community includes sea-ice-associated and pelagic organisms. The landfast ice is characterized by the high abundance of pennate diatoms (Poulin et al. 2011) and other groups during the ice melting period (e.g. prasinophytes, Mundy et al. 2011). The pelagic community includes diatoms, nano- and picoprasinophytes (especially *Micromonas pusilla*, Lovejoy et al. 2007) and other groups such as cryptophytes or haptophytes (Lovejoy et al. 2006, Balzano et al. 2012). Our results based on pigments are consistent with these observations.

Cell viability methods, when applied to natural communities, provide relevant information on phytoplankton responses to the environment. The CDA is a valuable method to quantify living cells in natural phytoplankton communities because it does not involve staining, and the optical and fluorescent signals of phytoplankton cells remained invariable after the CDA test, helping identification (Agustí & Sánchez 2002). However, the CDA provides valuable results only after quantification of total cell abundances in control samples (without enzymes) and of remaining living cells in samples exposed to the CDA enzymatic cocktail. Non-quantitative applications of the method as performed by Zetsche & Meysman (2012) or other results without detailed quantitative data are not appropriate uses of the CDA method. When microscopy methods are required to count and identify the natural populations, as in our study, application of the CDA method implies a notable effort and is time-consuming. As a quantitative method, the quality of the results when applying the CDA depends on the same aspects expected when quantifying phytoplankton, including the experience of the microscopist and the abundance and complexity of the communities in the water body tested (Dromph et al. 2013).

We observed a large variability in the %LC at both sets of stations. This agrees with already reported estimates of cell lysis rates in natural phytoplankton communities that show a large variability in time and space (Agustí et al. 1998, Agustí & Duarte 2000, Brussaard 2004). The averaged %LC values found during this study at OW and IC stations did not differ, and the range in %LC was very large, as observed by Lasternas & Agustí (2010) for Arctic communities. We observed a mean ± SE percentage of living cells in our study of 57.3 ± 5.8% for OW and 48.0 ± 3.9% for IC stations, which is in agreement with average viability data in other studies examining natural communities (e.g. Agustí 2004, Lasternas & Agustí 2014). Contrary to natural populations, phytoplankton growing in cultures show a higher % of living cells, close to 100% in the exponential phase (Agustí & Sánchez 2002). The optimized growth conditions in

cultures explain this difference between natural and cultured phytoplankton. The high viability together with the high cell abundance reached by phytoplankton in cultures also imply the need for a very precise quantification of the cell abundance when applying the CDA to cultured phytoplankton. This lack of quantification led Zetsche & Meysman (2012), by simply observing the large abundance of living cells after applying the CDA to phytoplankton cultures, to erroneously conclude that the CDA enzymes did not efficiently digest the cells. However, it is our opinion that this was a non-quantitative use of the CDA method involving erroneous interpretations (Zetsche & Meysman 2012). We validated the % of viable *Nitzschia frigida* cells obtained with the CDA against the % observed using a vital stain, and found significant agreement. We are thus confident in our results for the percentage of living cells in the natural environment of the Beaufort Sea.

The %LC was significantly and positively correlated with the photosynthetic performance index (F_v/F_m, Fig. 5a), which is a proxy for photoinhibition or downregulation of PSII (Critchley 2000). Hence a decrease in cell viability expressed as %LC was associated in our results with a decrease in photosynthetic performance as F_v/F_m.

The environmental variables examined (NO_3, irradiance and temperature) had a different association with the viability of phytoplankton cells, according to the group of stations considered. The distribution of %LC did not show a relationship with the concentration of nutrients, as expected from past studies in other oceanic regions (Agustí et al. 1998, Alonso-Laita & Agustí 2006, Lasternas et al. 2010). The lack of a relationship between the %LC distribution and nutrient concentrations in our results suggests that irradiance and water temperature were more important than nutrients in explaining the changes in the algal cell viability during the study (see Fig. 4).

Throughout the study, we investigated the influence of irradiance using the PAR at the sampling depth (E_z; Fig. 4a). We assumed that this parameter was representative of the environmental irradiance influencing the cells, as the *in situ* measurements were consistent with the daily incident irradiance measurements. Irradiance differently influenced the %LC at OW and IC stations; cells at OW stations were clearly exposed to much higher irradiances than cells at IC stations. Under low irradiances (<15 µmol photons m^{-2} s^{-1}), the highest %LC at IC stations matched with high percentages of diatoms, likely well acclimated to low irradiances, such as bottom ice pennate diatoms that are released and enter the water column. These diatom cells might be photoinhibited at higher irradiances (25–50 µmol photons m^{-2} s^{-1}, McMinn et al. 2007, Mangoni et al. 2009) with potential loss of viability (van de Poll et al. 2005). At higher irradiances (>15 µmol photons m^{-2} s^{-1}), %LC showed an increasing trend with irradiance at IC stations, along with a community formed of prasinophytes and diatoms likely able to cope with the increasing irradiances of the ice melting conditions (Petrou et al. 2011). These stations were located in landfast ice, while the ice cover was retreating or completely retreated (as for Stns F7 and FB07, 24–25 June) with the exception of Stn F5 (28 May, ~20% ice cover, see Fig. 1). For OW stations, the higher %LC values were associated with the diatom bloom in May. These communities showed a threshold of optimum irradiance at 600 µmol photons m^{-2} s^{-1} (Fig. 4a), showing a clear loss of viability at higher irradiances. This observation is consistent with photoinhibition at irradiances >600 µmol photons m^{-2} s^{-1} observed in other polar studies (van de Poll et al. 2005, Petrou & Ralph 2011). The significant loss of photosynthetic performance (F_v/F_m) with the increasing irradiance (E_{zm}, Fig. 5b) confirmed the detrimental physiological condition of the cells under these high irradiance OW conditions. Interestingly, the best relationship between the physiological condition of the cells (F_v/F_m) and the irradiance was obtained using E_{zm} instead of E_z. Our results showed the influence of water column stratification on the physiological performance of the cells. Since E_{zm} considers the changes of the surface mixed layer depth, this parameter might describe more accurately the irradiance that influenced the photosynthetic performance of the cells throughout the season.

The high-irradiance OW stations ($E_z \geq 600$ µmol photons m^{-2} s^{-1}) were characterized by low %LC (Fig. 4a) along with increased photoprotection potential compared to IC stations (see Table 2). Samples with increased photoprotection at these high irradiances showed a relatively high contribution of green algae (21% prasinophytes, 14% diatoms) compared to low-photoprotection, high-irradiance samples (4% prasinophytes, 34% diatoms). The highest PPC:PSC values measured at OW stations are similar to those found in communities dominated by green algae in other oceanic regions (Allali et al. 1997, Roy et al. 2008), whereas the lower values are comparable to those observed in other polar regions (Kropuenske et al. 2009, Petrou et al. 2011).

Photoprotection capacity might be a key factor explaining cell viability and the fact that this capacity differs among diatoms (Dimier et al. 2007, Lavaud et

al. 2007) might explain some of the variability in the %LC encountered during this study for *in situ* irradiances (E_z) lower than 600 µmol photons m^{-2} s^{-1}. This result could also be explained by the different photoprotective capacity between planktonic and sea-ice-associated algal cells that are released in the water column (Barnett et al. 2015). Values of (DD+DT):chl *a* above 0.4 wt:wt have been suggested to occur during nutrient limitation in Antarctic diatoms (van de Poll et al. 2005, van de Poll & Buma 2009). However, the shallowing of the surface mixed layer, the increase of the vertical stratification and the marked seasonal increase of daily irradiances probably exposed the cells to high irradiances (including potentially damaging UV) for longer periods (24 h day length), especially by the end of our study when irradiances and stratification were higher, likely causing the observed viability loss in diatoms. Unfortunately, nutrient concentrations were not always determined at the stations with the measured higher irradiances, making it difficult to determine whether there was a combined effect of nutrient limitation and excessive irradiance causing the observed loss of viability (van de Poll et al. 2005).

Within the ranges of water temperatures observed during the present study there was a combination of meltwater (−2 to 2°C) and pelagic (>2°C) communities occupying these distinct ecological niches (see Petrou & Ralph 2011). The ice-covered phytoplankton community showed responses in cell viability within a narrow variability in temperature (Fig. 4b), with a significant decrease of %LC above 0°C, with the lowest %LC stations being characterized by a community largely composed of prasinophytes. The bloom in the ice-covered community occurred when the ice melting accelerated and surface seawater temperature was around 0°C. The collapse of the bloom occurred in mid-June and was fast, parallel to the increase in temperatures and the drastic reduction of ice cover, and this was well reflected in the sharp decrease in viability at temperatures above 0°C (Fig. 4b). Phytoplankton at OW stations showed increased values of chl *a* in May, but did not show a clear bloom as observed in the IC area (Fig. 2c). At OW stations, light conditions were important in determining phytoplankton viability. In our study, F_v/F_m was variable (0.05–0.8) but did not show a good relationship with %LC at OW stations. However, high F_v/F_m values are not always evidence of the absence of dead cells (Franklin et al. 2009) and these values can vary widely in natural communities from polar environments (McMinn & Hegseth 2004). Some polar algae are able to acclimate to high temperatures (>7°C, Michel et al. 1989) with no influence on photosynthetic performance (F_v/F_m ~0.6, Petrou et al. 2012).

The degradation pigment pyropheophorbide *a*-'like' (relative to chl *a*) was the only pigment that showed a significant (inverse) relationship with both %LC and F_v/F_m (Fig. 5c,d). In contrast to some other studies (Llewellyn et al. 2008, Szymczak-Żyła et al. 2008), we did not find a clear relationship of %LC (or F_v/F_m) with chlorophyllide *a*, often considered a marker of cell senescence. In a recent study on cell senescence in the haptophyte *Emiliania huxleyi* and the diatom *Thalassiosira pseudonana*, Franklin et al. (2012) found species-specific senescence responses, which included increases in the pigment methoxychlorophyll *a* only in *T. pseudonana*. In the natural communities examined in the present study, the pigment pyropheophorbide *a*-'like' appears to be a good marker for senescence, more likely associated with the ice-covered community particularly during melting conditions, accounting for its positive correlation with the stratification index at these IC stations.

CONCLUSIONS

This study provides the first assessment of algal cell viability associated with environmental changes in the surface waters of the Beaufort Sea during the spring–summer transition. The %LC of phytoplankton varied widely, and this variation was related in part to changes in the community composition. The %LC was influenced by irradiance and temperature, showing distinct trends for OW and IC stations. Photosynthetic performance and %LC decreased with increasing irradiance, suggesting a detrimental effect of high irradiances on the physiological condition of phytoplankton. The lower %LC values were related to the highest irradiances at OW stations and to melting temperatures at IC stations. A pigment that we called pyropheophorbide *a*-'like' and that will need to be fully identified with appropriate techniques (such as liquid chromatography-mass spectrometry) shows potential as a marker pigment for the loss of cell viability in this environment. Based on the major marker pigments detected, diatoms seemed to thrive better than other groups during the spring–summer melting conditions. This may be because they occupy specific ecological niches with optimal biochemical and physical conditions in which they are favored, suggesting a certain degree of specialization over other microalgal cells.

Within the context of the continued global warming in the Arctic, our results suggest that phytoplankton physiological inter- and intra-specific differences could be key factors explaining the changes in community composition. The freshening of the surface waters as a result of sea-ice melting seems to favor the growth of planktonic diatoms over prasinophytes.

In a similar scenario than the one encountered by the end of this study (ice free, high irradiances and temperatures, highly stratified waters, and a shallow surface mixed layer), our results suggest a loss of cell viability when cells are exposed to high irradiances (>600 µmol photons m^{-2} s^{-1}). Extrapolating our results suggests that future increases in the surface mixed layer irradiance due to climate-related decreases in sea-ice coverage and thickness as well as increased water temperature may negatively affect the physiology of Arctic phytoplankton species, potentially reducing cell viability. This study highlights the complexity of the responses of natural communities submitted to different perturbation factors of the environment.

Acknowledgements. This work is a contribution to the International Polar Year-Circumpolar Flaw Lead system study (IPY-CFL 2008), supported through grants from the Canadian IPY Federal Program office and the Natural Sciences and Engineering Research Council (NSERC) of Canada. E.A.-F. received post-graduate scholarships from the Institut des sciences de la mer de Rimouski (ISMER) and Université du Québec à Rimouski and a stipend from Québec-Océan (through a grant from the Fonds de recherche du Québec – Nature et technologies). NSERC discovery grants to S.R. and to M.G. also helped to support this work. We thank the officers and crew of the CCGS 'Amundsen' for logistical support; and M. Palmer, J. Salcedo, M. Lionard, and M. Simard for assistance in the field and/or laboratory. We are grateful to P. Guillot for processing of CTD cast data; J. Gagnon for nutrient analysis; S. Lessard for algal counts and identification; Dr. T. Papakyriakou for providing incident PAR data; and 3 anonymous reviewers for their constructive comments on the manuscript. This is a contribution to the research programs of CFL, ArcticNet, ISMER, and Québec-Océan.

LITERATURE CITED

Agustí S (2004) Viability and niche segregation of *Prochlorococcus* and *Synechococcus* cells across the central Atlantic Ocean. Aquat Microb Ecol 36:53–59

Agustí S, Duarte CM (2000) Strong seasonality in phytoplankton cell lysis in the NW Mediterranean littoral. Limnol Oceanogr 45:940–947

Agustí S, Sánchez MC (2002) Cell viability in natural phytoplankton communities quantified by a membrane permeability probe. Limnol Oceanogr 47:818–828

Agustí S, Satta MP, Mura MP, Benavent E (1998) Dissolved esterase activity as a tracer of phytoplankton lysis: evidence of high phytoplankton lysis rates in the northwestern Mediterranean. Limnol Oceanogr 43:1836–1849

Agustí S, Alou E, Hoyer MV, Frazer TK, Canfield DE (2006) Cell death in lake phytoplankton communities. Freshw Biol 51:1496–1506

Allali K, Bricaud A, Claustre H (1997) Spatial variations in the chlorophyll-specific absorption coefficients of phytoplankton and photosynthetically active pigments in the equatorial Pacific. J Geophys Res 102:12413–12423

Alonso-Laita P, Agustí S (2006) Contrasting patterns of phytoplankton viability in the subtropical NE Atlantic Ocean. Aquat Microb Ecol 43:67–78

Alonso-Laita P, Navarro N, Duarte CM, Agustí S (2005) Seasonality of pico-phytoplankton abundance and cell death in a Mediterranean Bay (Bay of Palma, Majorca Island). Vie Milieu 55:177–184

Alou-Font E (2013) Viabilité du phytoplancton et des algues de glace dans la mer de Beaufort (Arctique canadien). PhD thesis, Université du Québec à Rimouski

Arrigo KR, van Dijken G, Pabi S (2008) Impact of a shrinking ice cover on marine primary production. Geophys Res Lett 35:L19603, doi:10.1029/2008GL035028

Balzano S, Marie D, Gourvil P, Vaulot D (2012) Composition of the summer photosynthetic pico and nanoplankton communities in the Beaufort Sea assessed by T-RFLP and sequences of the 18S rRNA gene from flow cytometry sorted samples. ISME J 6:1480–1498

Barber DG, Asplin MG, Gratton Y, Lukovich J, Galley RJ, Raddatz RL, Leitch D (2010) The International Polar Year (IPY) Circumpolar Flaw Lead (CFL) system study: overview and the physical system. Atmos-Ocean 48:225–243

Barnett A, Méléder V, Blommaert L, Lepetit B and others (2015) Growth form defines physiological photoprotective capacity in intertidal benthic diatoms. ISME J 9:32–45

Bidigare RR, Van Heukelem L, Trees CC (2005) Analysis of algal pigments by high-performance liquid chromatography. In: Andersen RA (ed) Algal culturing techniques. Elsevier Academic Press, Amsterdam, p 327–345

Brown TA, Belt ST, Philippe B, Mundy CJ, Massé G, Poulin M, Gosselin M (2011) Temporal and vertical variations of lipid biomarkers during a bottom ice diatom bloom in the Canadian Beaufort Sea: further evidence for the use of the IP25 biomarker as a proxy for spring Arctic sea ice. Polar Biol 34:1857–1868

Brussaard CPD (2004) Viral control of phytoplankton populations — a review. J Eukaryot Microbiol 51:125–138

Brzezinski MA (1985) The Si:C:N ratio of marine diatoms: interspecific variability and the effect of some environmental variables. J Phycol 21:347–357

Carmack EC, Macdonald RW (2002) Oceanography of the Canadian Shelf of the Beaufort Sea: a setting for marine life. Arctic 55:29–45

Coello-Camba A, Agustí S, Holding J, Arrieta JM, Duarte CM (2014) Interactive effect of temperature and CO_2 increase in Arctic phytoplankton. Front Mar Sci 1:49, doi: 10.3389/fmars.2014.00049

Comiso JC, Parkinson CL, Gersten R, Stock L (2008) Accelerated decline in the Arctic sea ice cover. Geophys Res Lett 35:L01703, doi:10.1029/2007GL031972

Critchley C (2000) Photoinhibition. In: Raghavendra AS (ed) Photosynthesis — a comprehensive treatise. Cambridge University Press, Cambridge, p 264–272

de Boyer Montégut C, Madec G, Fischer AS, Lazar A, Iudicone D (2004) Mixed layer depth over the global ocean: an examination of profile data and a profile-based climatology. J Geophys Res 109:C12003, doi:10.1029/2004JC002378

Dimier C, Corato F, Tramontano F, Brunet C (2007) Photoprotection and xanthophyll-cycle activity in three marine diatoms. J Phycol 43:937–947

Dromph KM, Agustí S, Basset A, Franco J and others (2013) Sources of uncertainty in assessment of marine phytoplankton communities. Hydrobiologia 704:253–264

Echeveste P, Agustí S, Dachs J (2011) Cell size dependence of additive versus synergetic effects of UV radiation and PAHs on oceanic phytoplankton. Environ Pollut 159:1307–1316

Egeland ES, Garrido JL, Clementson L, Andresen K and others (2011) Data sheets aiding identification of phytoplankton carotenoids and chlorophylls. In: Roy S, Llewellyn CA, Egeland ES, Johnsen G (eds) Phytoplankton pigments: characterization, chemotaxonomy and applications in oceanography. Cambridge University Press, Cambridge, p 257–301

Forest A, Tremblay JÉ, Gratton Y, Martin J and others (2011) Biogenic carbon flows through the planktonic food web of the Amundsen Gulf (Arctic Ocean): a synthesis of field measurements and inverse modeling analyses. Prog Oceanogr 91:410–436

Franklin DJ, Choi CJ, Hughes C, Malin G, Berges JA (2009) Effect of dead phytoplankton cells on the apparent efficiency of photosystem II. Mar Ecol Prog Ser 382:35–40

Franklin DJ, Airs RL, Fernandes M, Bell TG, Bongaerts RJ, Berges JA, Malin G (2012) Identification of senescence and death in *Emiliania huxleyi* and *Thalassiosira pseudonana*: cell staining, chlorophyll alterations, and dimethylsulfoniopropionate (DMSP) metabolism. Limnol Oceanogr 57:305–317

Garvey M, Moriceau B, Passow U (2007) Applicability of the FDA assay to determine the viability of marine phytoplankton under different environmental conditions. Mar Ecol Prog Ser 352:17–26

Gosselin M, Legendre L, Therriault JC, Demers S (1990) Light and nutrient limitation of sea-ice microalgae (Hudson Bay, Canadian Arctic). J Phycol 26:220–232

Grasshoff K, Kremling K, Ehrhardt M (1999) Methods of seawater analysis, 3rd edn. Wiley-VCH, New York, NY

Hayakawa M, Suzuki K, Saito H, Takahashi K, Ito SI (2008) Differences in cell viabilities of phytoplankton between spring and late summer in the northwest Pacific Ocean. J Exp Mar Biol Ecol 360:63–70

Hernando M, Schloss IR, Malanga G, Almandoz GO, Ferreyra GA, Aguiar MB, Puntarulo S (2015) Effects of salinity changes on coastal Antarctic phytoplankton physiology and assemblage composition. J Exp Mar Biol Ecol 466:110–119

Higgins HW, Wright SW, Schlüter L (2011) Quantitative interpretation of chemotaxonomic pigment data. In: Roy S, Llewellyn CA, Egeland ES, Johnsen G (eds) Phytoplankton pigments: characterization, chemotaxonomy and applications in oceanography. Cambridge University Press, Cambridge, p 257–301

Hill V, Cota G, Stockwell D (2005) Spring and summer phytoplankton communities in the Chukchi and eastern Beaufort Seas. Deep-Sea Res II 52:3369–3385

Horner R, Schrader GC (1982) Relative contributions of ice algae, phytoplankton, and benthic microalgae to primary production in nearshore regions of the Beaufort Sea. Arctic 35:485–503

Jeffrey SW (1997) Chlorophyll and carotenoid extinction coefficients. In: Jeffrey SW, Mantoura RFC, Wright SW (eds) Phytoplankton pigments in oceanography. UNESCO Publishing, Paris, p 595–596

Jochem FJ (2000) Probing the physiological state of phytoplankton at the single-cell level. Sci Mar 64:183–195

Kropuenske LR, Mills MM, van Dijken GL, Bialey S, Robinson DH, Welschmeyer NA, Arrigo KR (2009) Photophysiology in two major Southern Ocean phytoplankton taxa: photoprotection in *Phaeocystis antarctica* and *Fragilariopsis cylindrus.* Limnol Oceanogr 54:1176–1196

La Rocca N, Sciuto K, Meneghesso A, Moro I, Rascio N, Morosinotto T (2015) Photosynthesis in extreme environments: responses to different light regimes in the Antarctic alga *Koliella antarctica.* Physiol Plant 153:654–667

Lasternas S, Agustí S (2010) Phytoplankton community structure during the record Arctic ice-melting of summer 2007. Polar Biol 33:1709–1717

Lasternas S, Agustí S (2014) The percentage of living bacterial cells related to organic carbon release from senescent oceanic phytoplankton. Biogeosciences 11: 6377–6387

Lasternas S, Agustí S, Duarte CM (2010) Phyto- and bacterioplankton abundance and viability and their relationship with phosphorus across the Mediterranean Sea. Aquat Microb Ecol 60:175–191

Lavaud J, Strzepek RF, Kroth PG (2007) Photoprotection capacity differs among diatoms: possible consequences on the spatial distribution of diatoms related to fluctuations in the underwater light climate. Limnol Oceanogr 52:1188–1194

Li WKW, McLaughlin FA, Lovejoy C, Carmack EC (2009) Smallest algae thrive as the Arctic Ocean freshens. Science 326:539

Llabrés M, Agustí S (2008) Extending the cell digestion assay to quantify dead phytoplankton cells in cold and polar waters. Limnol Oceanogr Methods 6:659–666

Llabrés M, Agustí S (2010) Effects of ultraviolet radiation on growth, cell death and the standing stock of Antarctic phytoplankton. Aquat Microb Ecol 59:151–160

Llewellyn CA, Tarran GA, Galliene CP, Cummings DG and others (2008) Microbial dynamics during the decline of a spring diatom bloom in the Northeast Atlantic. J Plankton Res 30:261–273

Lovejoy C, Massana R, Pedrós-Alió C (2006) Diversity and distribution of marine microbial eukaryotes in the Arctic Ocean and adjacent seas. Appl Environ Microbiol 72: 3085–3095

Lovejoy C, Vincent WF, Bonilla S, Roy S and others (2007) Distribution, phylogeny, and growth of cold-adapted picoprasinophytes in Arctic seas. J Phycol 43:78–89

Lund JWG, Kipling C, LeCren ED (1958) The inverted microscope method of estimating algal number and the statistical basis of estimations by counting. Hydrobiologia 11:143–170

Macdonald RW, Sakshaug E, Stein R (2004) The Arctic Ocean: modern status and recent climate change. In: Stein R, Macdonald RW (eds) The organic carbon cycle in the Arctic Ocean. Springer, Berlin, p 6–20

Mangoni O, Carrada GC, Modigh M, Catalano G, Saggiomo V (2009) Photoacclimation in Antarctic bottom ice algae: an experimental approach. Polar Biol 32:325–335

McMinn A, Hegseth EN (2004) Quantum yield and photosynthetic parameters of marine microalgae from the southern Arctic Ocean, Svalbard. J Mar Biol Assoc UK 84:865–871

McMinn A, Ryan KG, Ralph PJ, Pankowski A (2007) Spring sea ice photosynthesis, primary productivity and biomass distribution in eastern Antarctica, 2002–2004. Mar Biol 151:985–995

Michel C, Legendre L, Therriault JC, Demers S (1989) Photosynthetic responses of Arctic Sea Ice microalgae to short-term temperature acclimation. Polar Biol 9: 437–442

Mundy CJ, Gosselin M, Ehn JK, Gratton Y and others (2009) Contribution of under-ice primary production to an ice-edge upwelling phytoplankton bloom in the Canadian Beaufort Sea. Geophys Res Lett 36:L17601, doi:10.1029/2009GL038837

Mundy CJ, Gosselin M, Ehn JK, Belzile C and others (2011) Characteristics of two distinct high-light acclimated algal communities during advanced stages of sea ice melt. Polar Biol 34:1869–1886

Overland JE, Wang M (2013) When will the summer Arctic be nearly sea ice free? Geophys Res Lett 40:2097–2101

Peterson BJ, Holmes RM, McClelland JW, Vörösmarty CJ and others (2002) Increasing river discharge to the Arctic Ocean. Science 298:2171–2173

Peterson BJ, McClelland J, Curry R, Holmes RM, Walsh JE, Aagaard K (2006) Trajectory shifts in the Arctic and subarctic freshwater cycle. Science 313:1061–1066

Petrou K, Ralph PJ (2011) Photosynthesis and net primary productivity in three Antarctic diatoms: possible significance for their distribution in the Antarctic marine ecosystem. Mar Ecol Prog Ser 437:27–40

Petrou K, Hill R, Doblin MA, McMinn A, Johnson R, Wright SW, Ralph PJ (2011) Photoprotection of sea-ice microalgal communities from the east Antarctic pack ice. J Phycol 47:77–86

Petrou K, Kranz SA, Doblin MA, Ralph PJ (2012) Photophysiological responses of *Fragilariopsis cylindrus* (Bacillariophyceae) to nitrogen at two temperatures. J Phycol 48:127–136

Poulin M, Daugbjerg N, Gradinger R, Ilyash L, Ratkova T, von Quillfeldt CH (2011) The pan-Arctic biodiversity of marine pelagic and sea-ice unicellular eukaryotes: a first-attempt assessment. Mar Biodivers 41:13–28

Rajanahally MA, Sim D, Ryan KG, Convey P (2014) Can bottom ice algae tolerate irradiance and temperature changes? J Exp Mar Biol Ecol 461:516–527

Redfield AC, Ketchum BH, Richards FA (1963) The influence of organisms on the composition of sea-water. In: Hill MN (ed) The sea, Vol 2. Interscience Publishers, New York, NY, p 26–77

Riley GA (1957) Phytoplankton of the north central Sargasso Sea 1950–52. Limnol Oceanogr 2:252–270

Roy S, Legendre L (1979) DCMU-enhanced fluorescence as an index of photosynthetic activity in phytoplankton. Mar Biol 55:93–101

Roy S, Blouin F, Jacques A, Therriault JC (2008) Absorption properties of phytoplankton in the Lower Estuary and Gulf of St. Lawrence (Canada). Can J Fish Aquat Sci 65: 1721–1737

Rózanska M, Gosselin M, Poulin M, Wiktor JM, Michel C (2009) Influence of environmental factors on the development of bottom ice protist communities during the winter–spring transition. Mar Ecol Prog Ser 386:43–59

Rysgaard S, Nielsen TG, Hansen BW (1999) Seasonal variation in nutrients, pelagic primary production and grazing in a high-arctic coastal marine ecosystem, Young Sound, Northeast Greenland. Mar Ecol Prog Ser 179:13–25

Spooner N, Keely BJ, Maxwell JR (1994) Biologically mediated defunctionalization of chlorophyll in the aquatic environment — I. Senescence/decay of the diatom *Phaeodactylum tricornutum*. Org Geochem 21:509–516

Stroeve J, Holland MM, Meier W, Scambos T, Serreze M (2007) Arctic sea ice decline: faster than forecast. Geophys Res Lett 34:L09501, doi:10.1029/2007GL029703

Szymczak-Żyła M, Kowalewska G, Louda JW (2008) The influence of microorganisms on chlorophyll *a* degradation in the marine environment. Limnol Oceanogr 53: 851–862

Tremblay JÉ, Gagnon J (2009) The effects of irradiance and nutrient supply on the productivity of Arctic waters: a perspective on climate change. In: Nihoul JCJ, Kostianoy AG (eds) Influence of climate change on the changing Arctic and subarctic conditions. Springer, Dordrecht, p 73–93

Tremblay JÉ, Bélanger S, Barber DG, Asplin M and others (2011) Climate forcing multiplies biological productivity in the coastal Arctic Ocean. Geophys Res Lett 38:LI8604, doi:10.1029/2011GL048825

Tremblay JÉ, Robert D, Varela DE, Lovejoy C, Darnis G, Nelson RJ, Sastri AR (2012) Current state and trends in Canadian Arctic marine ecosystems: I. Primary production. Clim Change 115:161–178

Van Boekel WHM, Hansen FC, Riegman R, Bak RPM (1992) Lysis-induced decline of a *Phaeocystis* spring bloom and coupling with the microbial foodweb. Mar Ecol Prog Ser 81:269–276

Van de Poll WH, Buma AGJ (2009) Does ultraviolet radiation affect the xanthophyll cycle in marine phytoplankton? Photochem Photobiol Sci 8:1295–1301

Van de Poll WH, Van Leeuwe MA, Roggeveld J, Buma AGJ (2005) Nutrient limitation and high irradiance acclimation reduce PAR and UV-induced viability loss in the Antarctic diatom *Chaetoceros brevis* (Bacillariophyceae). J Phycol 41:840–850

Wang J, Cota GF, Comiso JC (2005) Phytoplankton in the Beaufort and Chukchi Seas: distribution, dynamics, and environmental forcing. Deep-Sea Res II 52:3355–3368

Zapata M, Rodríguez F, Garrido JL (2000) Separation of chlorophylls and carotenoids from marine phytoplankton: a new HPLC method using a reversed phase C_8 column and pyridine-containing mobile phases. Mar Ecol Prog Ser 195:29–45

Zetsche EV, Meysman FJR (2012) Dead or alive? Viability assessment of micro- and mesoplankton. J Plankton Res 34:493–509

Zhang J, Spitz YH, Steele M, Ashjian C, Campbell R, Berline L, Matrai M (2010) Modeling the impact of declining sea ice on the Arctic marine planktonic ecosystem. J Geophys Res 115:C10015, doi:10.1029/2009JC005387

Editorial responsibility: Graham Savidge, Portaferry, UK

Submitted: January 28, 2015; Accepted: November 19, 2015
Proofs received from author(s): January 26, 2016